PHYSICAL REVIEW A VOLUME 26, NUMBER 3 SEPTEMBER 1982

Influence of an applied electric field on state changing in xenon-Rydberg-atom—xenon collisions

M. P. Slusher, C. Higgs, K. A. Smith, F. B. Dunning, and R. F. Stebbings
Department of Space Physics and Astronomy and Rice Quantum Institute, Rice University, Houston, Texas 77251
(Received 17 August 1981)

The influence of an applied electric field on state changing in collisions between laser-excited Xe(nf) atoms and xenon target gas is described. The presence of the field results in marked changes in both the rate constant for collisional state changing and the final-state distribution. The changes can be generally understood in terms of energy-transfer arguments based on the "essentially-free" electron model, although the degree of spatial overlap between the wave functions associated with the initial and final states may also be important.

I. INTRODUCTION

In recent years many studies of state changing in thermal collisions between Rydberg atoms and various atomic and molecular targets have been reported.[1–8] These studies were undertaken in near-zero electric fields. However, atoms in high Rydberg states are significantly perturbed by even relatively small electric fields such as are present in many environments, e.g., plasmas, where collisions occur. It is therefore of interest to study the influence of an applied dc electric field on state-changing collisions. In this paper we describe the results of such an investigation, considering as a specific example Xe(31f)-Xe collisions.[9] The collision products are analyzed by selective field ionization (SFI).[5] The data show that the presence of even a modest applied dc electric field results in marked changes in both the rate constant for collisional state changing and in the final-state distribution. These changes are consistent with those expected from consideration of energy-transfer arguments based on the "essentially-free" electron model. However, the data also suggest that the spatial overlap between the wave functions associated with the initial and final states may be important.

II. EXPERIMENTAL

The experimental apparatus has been described in detail elsewhere[1] and will be only briefly discussed. A beam containing xenon metastable atoms is directed into an interaction region, which is located between two parallel mesh grids, and which contains xenon target gas at a pressure of $\sim 2\times 10^{-5}$ Torr. A fraction of the metastable atoms is photoexcited, in zero electric field, to a selected nf level by use of a tunable N_2-pumped dye laser. Immediately (<1 μsec) following excitation, a dc electric field is established across the interaction region by application of a suitable potential to the upper interaction-region grid. Collisions are then allowed to occur in the presence of this field for a selected time interval, typically in the range 1—8 μsec, whereupon the excited atoms present in the interaction region are analyzed by SFI. To accomplish this a ramped potential is applied to the lower interaction-region grid causing the electric field in the interaction region to increase to ~ 1400 V cm^{-1} in ~ 1 μsec. The electrons liberated by field ionization are detected by a particle multiplier whose output is fed to a time-to-amplitude converter (TAC). The TAC is started at the beginning of the ionizing ramp and stopped by the first pulse subsequently registered by the detector. The TAC output is stored in a multichannel analyzer (MCA). For sufficiently low count rates the MCA signal is proportional to the probability of a field ionization event per unit time during the voltage ramp. Measurement of the time dependence of the ionizing field then enables the field dependence of the ionization signal to be determined.

Because atoms in different Rydberg states ionize at different electric field strengths, it is, in principle, possible to infer from such SFI data the state distribution of the excited reaction products. However, such an analysis requires a detailed understanding of how the atoms respond as the ionizing field is increased, because a given ionization feature

can only be attributed to atoms in a particular initial Rydberg state if the details of the path to ionization are known.

Field ionization has been discussed in detail by several authors.[1,10–16] However, as an aid to interpreting the present data, a brief review of the essential characteristics of field ionization is included here. The process will be discussed by reference to Fig. 1, which shows the $m_l=0$ Stark states of hydrogen in the vicinity of $n=15$.[17] As illustrated in the inset, application of an electric field results in the formation of a saddle point in the potential experienced by the Rydberg electron. Classically, ionization can occur whenever the Stark shifted energy of a state lies at, or above, this saddle point. The line labeled V_{SAD} shows the height of the saddle point as a function of applied field and thus separates the region, to the right, where ionization is classically possible from that, to the left, where it is not. Quantum mechanical treatments of field ionization, however, indicate that the hydrogenic Stark states shown in Fig. 1 have appreciable ionization rates ($\gtrsim 10^7$ sec^{-1}) only in the dashed regions.[18] It is evident that the higher-lying Stark states in each n manifold remain relatively stable in fields where, classically, they are unstable. This is a consequence of the low electron probability densities associated with these states in the vicinity of the saddle point.[1,5]

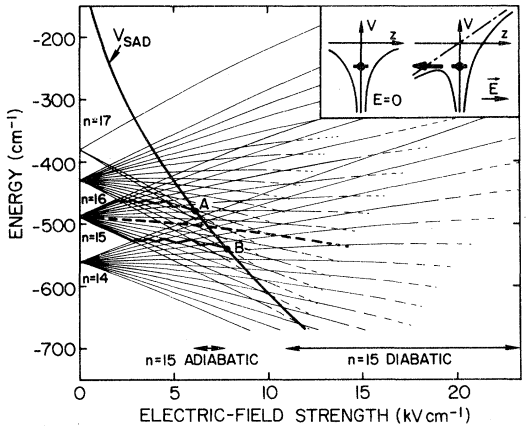

FIG. 1. Hydrogenic $m_l=0$ Stark states in the vicinity of $n=15$. The high-field region of each state is dashed to indicate the range of field strengths over which the ionization rate increases from $\sim 10^7$ to 10^{11} sec^{-1}. The heavy solid lines give examples of adiabatic passage to ionization; the heavy dashed line is an example of diabatic passage. In the inset is shown the potential energy of the Rydberg electron in the absence and the presence of an external electric field directed along the z axis. The height of the resultant saddle point as a function of the applied field is shown by the line labeled V_{SAD}.

In the case of multielectron atoms such as xenon, the response to an electric field is complicated by the presence of non-Coulombic terms in the Hamiltonian. These terms lead to interactions between states of the same $|m_l|$ and result in avoided crossings whenever states of the same $|m_l|$ in different Stark manifolds approach one another. Nonetheless, except for the presence of these avoided crossings, the general Stark structure for complex atoms is similar to that for hydrogen,[19] and the ionization of such atoms can be discussed using energy levels and ionization rates calculated using hydrogenic theory.

The ionization characteristics of a complex atom depend critically upon its behavior at avoided crossings. If the atom is in a state that is not strongly coupled to other states the energy separation at avoided crossings is small. If the field is then increased sufficiently rapidly, there is a high probability that the avoided crossings will be traversed diabatically. The atom remains in a single Stark state and follows a "diabatic" path to ionization such as that shown by the heavy dashed line in Fig. 1. Diabatic ionization of $m_l=0$ states in the $n=15$ manifold will thus occur over the range of field strengths marked "diabatic" in Fig. 1. On the other hand, if the atom is in a state that interacts strongly with states from other manifolds the energy separations at avoided crossings are large. If then the rate of increase, i.e., slew rate, of the ionizing field is sufficiently low, there is a high probability that the avoided crossings will be traversed adiabatically. Atoms will then follow paths to ionization such as those shown by the heavy solid lines in Fig. 1. They thus successively assume the character of many different Stark states. All atoms in $n=15$ $m_l=0$ states that follow such "adiabatic" paths to ionization cross the saddle-point line V_{SAD} between A and B. To the right of this line the atoms experience a dramatic increase in ionization probability due to their interaction with the lower members of higher Stark manifolds, which are highly unstable against ionization in this region. They therefore ionize at field strengths close to those predicted by classical saddle-point theory in the range marked adiabatic in Fig. 1.

Previous studies have shown that Rydberg atoms typically follow either predominantly adiabatic or predominantly diabatic paths to ionization, although under certain conditions an atom may exhibit a combination of adiabatic and diabatic behavior at avoided crossings during passage to ionization. The probability of diabatic passage increases with n,

$|m_l|$, and the slew rate of the ionizing field. For $n \sim 30$, and the present slew rates of $\sim 10^9$ V cm^{-1} sec^{-1}, xenon atoms with $|m_l| < 4$ ionize predominantly adiabatically, while those with $|m_l| \geq 4$ ionize predominantly diabatically.[1,3,4]

III. RESULTS AND DISCUSSION

SFI spectra obtained following collisions of laser-excited Xe($31f$) atoms with xenon target gas at a pressure of 2×10^{-5} Torr in various applied dc electric fields in the range 0–91 V cm^{-1} are shown in Figs. 2(a)–2(f). Each spectrum results from the same number of laser-excited atoms. The arrows shown beneath the data indicate the ranges of electric field strengths over which adiabatic and diabatic ionization of xenon atoms in $n=31$ states occurs.

In the absence of target gas a single relatively sharp ionization feature is observed as shown in Fig. 2(g). This results from the predominantly adiabatic ionization of the laser-excited atoms.[1,3] The data in Fig. 2(g) are characteristic of the SFI spectra observed for all applied dc fields in the absence of target gas.

Introduction of target gas leads to the appearance of SFI features, labeled P_1 and P_2, at field strengths that correspond to diabatic ionization. SFI data similar to those obtained in zero applied field, Fig. 2(a), have been discussed previously.[4] The feature P_0 results from ionization of remaining parent atoms plus the low-$|m_l|$ products of l-changing collisions that ionize adiabatically. The feature P_1 results from the $|m_l| \geq 4$, diabatically ionizing products of such collisions. No SFI features resulting from ionization of the products of n-changing collisions are detected, nor is there evidence of collisional ionization. The collisionally induced diabatic ionization signals, obtained by removal of the underlying background due to ionization of remaining parent $31f$ atoms, are shown on an expanded scale in Fig. 3. The profile, and width, of the collisionally induced diabatic ionization signal observed following collisions in zero field [Fig. 3(a)] is similar to that calculated for diabatic ionization of a mixture containing equal numbers of atoms in each $n=31$, $|m_l| \geq 4$ Stark state. The calculated profile, obtained as described elsewhere,[3,5] is shown in Fig. 4(b) for an electric field slew rate of 10^9 V cm^{-1} sec^{-1}. The extreme members of the $n=31$, and $n=30$, $|m_l|=4$ manifolds are shown[17] in Fig. 4(a) together with a series of points, each of which represents the location at which one of the

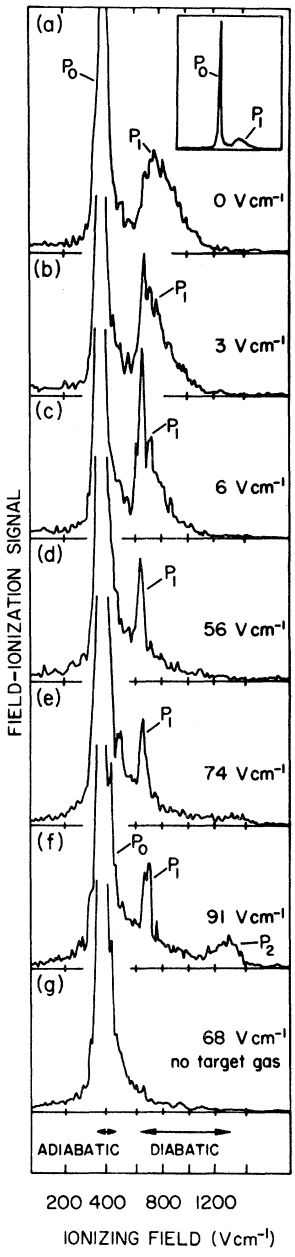

FIG. 2. SFI spectra obtained following the interaction for 8 μsec of laser-excited Xe($31f$) atoms with xenon target gas at a pressure of 2×10^{-5} Torr in the presence of applied dc fields in the range 0–91 V cm^{-1}. The data are for equal initial $31f$ populations. The inset in (a) indicates the relative sizes of the features P_0, P_1 resulting from adiabatic and diabatic ionization, respectively. The spectrum in (g) is obtained in the absence of target gas. The arrows indicate the ranges of ionizing field strengths over which $n=31$ states are expected to ionize adiabatically and diabatically.

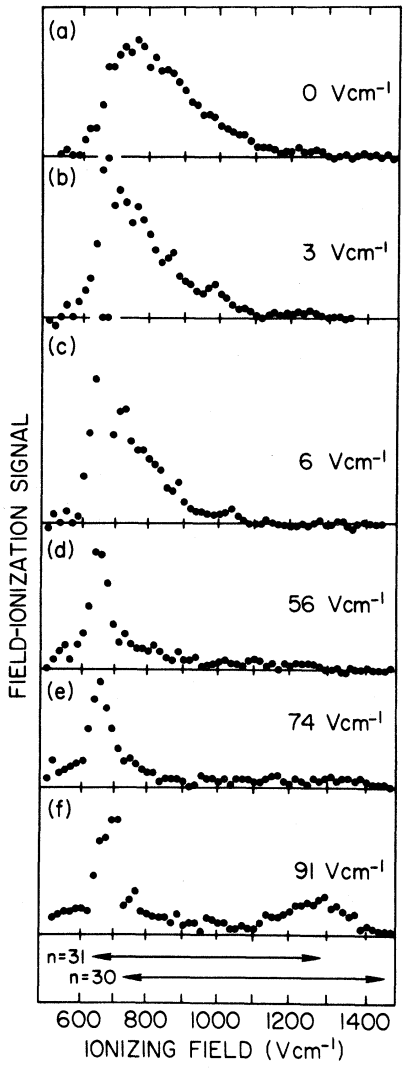

FIG. 3. Collisionally induced diabatic ionization features observed following collisions of laser-excited Xe(31f) atoms with xenon target gas at a pressure of 2×10^{-5} Torr for 8 μsec in the presence of several applied dc fields. The arrows indicate the ranges of ionizing field strengths over which $n=30$ and 31 states are expected to ionize diabatically.

$|m_l| \geq 4$ Stark states achieves an ionization rate of 10^9 sec^{-1}.[18] The similarity between the calculated and observed profiles indicates that, in zero field, collisions populate levels that evolve into states that have a broad range of values of l and $|m_l|$.[20]

The presence of even a modest dc electric field during the time collisions occur results in changes in the distribution of collisionally populated states. This is evidenced by the observed changes in the SFI spectra, which are particularly marked in the case of the diabatic features. For this reason, the present discussion will focus on the collisionally populated states that give rise to these features. The changes in the diabatic features can be explained qualitatively by appealing to the essentially-free electron model,[21] which assumes that the average separation between the Rydberg electron and its ionic core is so large that the target particle does not interact with both electron and core simultaneously. The Rydberg electron thus behaves as if it were free, except that it has a momentum distribution determined by its quantum state. The collision is then discussed by considering the electron-target and core-target interactions separately. Previous studies in zero applied field[4] have shown that, for Xe(nf)-Xe collisions, effects due to the core are so small that such interactions are well described by considering only the Rydberg electron-target interaction. The amount of energy that can be transferred to or from a Rydberg atom during a Xe(nf)-Xe collision can thus be determined by considering the kinematics of an elastic collision between the Rydberg electron and the target atom. The energy transfer depends on the relative Rydberg electron-target velocity and the electron scattering angle. Calculation of the average energy transfer, and the relative probabilities for different energy transfers, is, however, difficult as this requires averaging over all possible initial relative velocities and impact parameters. Thus to obtain an *estimate* of the energy transfer we consider the special case of "head-on" collisions between the Rydberg electron and the xenon target atom, i.e., collisions in which the xenon atom is moving directly toward (or away from) the Rydberg electron. If it is assumed that the Rydberg electron is isotropically scattered, then consideration of the collision dynamics shows that, if the electron velocity is taken to be that corresponding to its time-averaged kinetic energy and if the Xe(nf)-Xe relative collision velocity is taken to be the average thermal velocity, the average energy transfer will be ~0.9 cm^{-1}. However, because the majority of Rydberg electron-target collisions are not head-on and because, for large impact parameters, the xenon target atom will sample only the low-velocity region of the Rydberg electron velocity distribution, energy transfers that are smaller than this value will be favored. Thus, the essentially-free electron model suggests that only Rydberg states having energies within ~0.9 cm^{-1} of the parent level should be readily accessible through collisions. This range of energies is indicated by the dotted region in the inset in Fig. 4(a) which shows, on an expanded scale, the adiabatic evolution of the $m_l=0$ state resulting

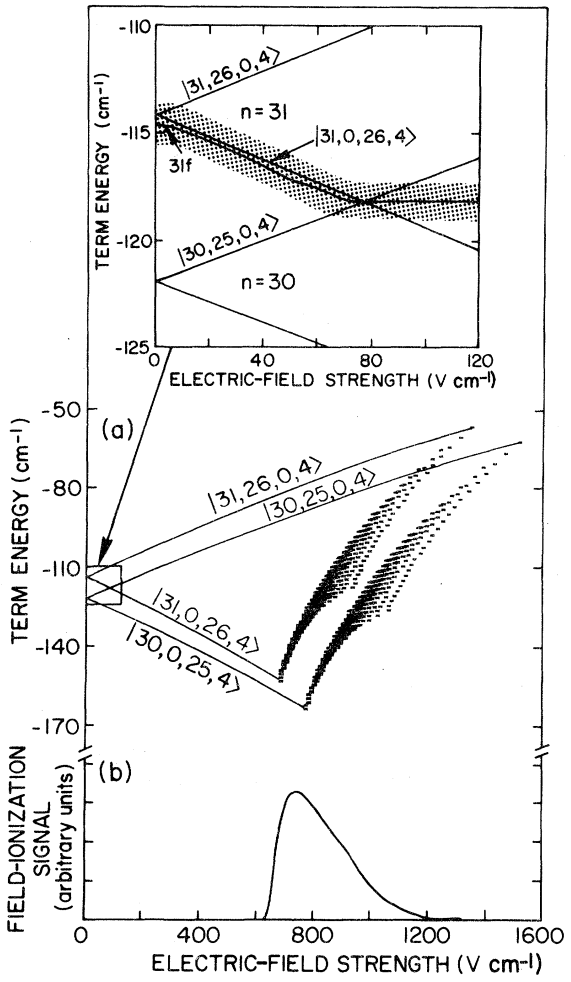

FIG. 4. (a) Partial energy level diagram for xenon Rydberg states. The solid lines represent the extreme members of the $n=30,31$ $|m_l|=4$ manifolds. Each cross represents the location at which one $|m_l| \geq 4$ Stark state achieves an ionization rate of 10^9 sec^{-1}. The SFI profile calculated for diabatic ionization of a mixture containing equal numbers of atoms in each $|m_l| \geq 4$ $n=31$ Stark state at a slew rate of 10^9 V cm^{-1} sec^{-1} is shown in (b). The inset shows, on an expanded scale, the adiabatic evolution of the $m_l=0$ state associated with the parent $31f$ state with increasing applied field, together with a shaded region which extends 0.9 cm^{-1} to either side.

from $31f$ excitation. This is similar to the lower of the two adiabatic paths indicated in Fig. 1. The $|m_l|=1$, 2, and 3 states resulting from $31f$ excitation evolve along paths immediately above that followed by the $m_l=0$ state. Also included in the inset are the extreme members of the $n=30,31$, $|m_l|=4$ Stark manifolds. Other diabatically ionizing, $|m_l| \geq 4$, $n=30,31$ Stark states lie between the extreme $|m_l|=4$ states.

It is seen from Fig. 4 that, in zero applied field, the $31f$ level lies sufficiently close to the $n=31$ manifold that all Stark states are energetically accessible. The broad collisionally induced diabatic ionization feature which is observed in zero fields [Fig. 3(a)] is thus to be expected. Application of an electric field of a few volts per centimeter leads to an *increased* energy separation between the higher-lying Stark states and the parent levels, together with a *decreased* separation between the parent and the low-lying Stark states. Thus, because the collision kinematics favor small energy transfers, the presence of a weak field would be expected to enhance the production of high-lying states. These trends are apparent in Figs. 3(b) and 3(c) which show a narrowing of the collisionally induced diabatic ionization feature toward ionizing field strengths that, as apparent from Fig. 4, correspond to diabatic ionization of the lower $|m_l| \geq 4$ members of the $n=31$ manifold. As the applied electric field is further increased fewer and fewer of the low-lying Stark states remain energetically accessible, leading to the very narrow diabatic ionization signals evident in Figs. 3(d) and 3(e). However, at sufficiently high fields, states from the $n=30$ and $n=31$ manifolds overlap, and a few states in both manifolds are energetically accessible. The collisionally induced diabatic ionization feature obtained under these conditions is shown in Fig. 3(f). Ionization of low-lying $n=31$, $|m_l| \geq 4$ Stark states gives rise to the ionization signal at ~ 680 V cm^{-1}, while the signal at ~ 1300 V cm^{-1} is attributed to ionization of high-lying $n=30$, $|m_l| \geq 4$ states.

Because collisional ionization and collisional transfer to other than neighboring levels are not observed, the number $n(t)$ of atoms comprising the adiabatic ionization feature P_0 at time t may be represented, under single collision conditions, by

$$n(t)=n(0)\exp-\left[\frac{1}{\tau_{\text{eff}}}+\rho k^{A\to D}\right]t\ ,$$

where $k^{A\to D}$ is the rate constant for collisional mixing to diabatically ionizing $|m_l| \geq 4$ states (ionization of $|m_l|<4$ collision products is included in P_0), $n(0)$ is the initial ($t=0$) population in P_0, and ρ is the target gas density. τ_{eff}, the effective lifetime of the parent atoms, depends on the strength of the applied field and is measured in a subsidiary experiment by observing the decay of the parent atoms in the absence of target gas. $k^{A\to D}$ may thus be determined, at various applied dc fields, from measure-

ments of $n(t)$ and the resulting values are shown in Fig. 5. Since $k^{A\to D}$ pertains to the collisional production of states with $|m_l| \geq 4$ it only affords a lower limit to the total rate constant for state changing. No estimate of the rate constant for mixing to low-$|m_l|$ states is obtained because it is not found possible to adequately resolve the separate contributions to P_0 that result from ionization of parent atoms and of low-$|m_l|$ collision products.

As evident from Fig. 5, $k^{A\to D}$ decreases markedly with increasing applied dc field. Two factors may be important in determining the field dependence of $k^{A\to D}$, namely the number of energetically accessible states and the degree of spatial overlap between the wave functions describing the initial and final states. The inset in Fig. 5 indicates how the number N_A of energetically accessible $|m_l| \geq 4$ Stark states that lie within 0.9 cm^{-1} of the parent levels varies with applied field, assuming that the $|m_l| = 0$, 1, 2, and 3 levels resulting from $31f$ excitation are statistically populated. The similarity between the behavior of this number of states and the measured values of $k^{A\to D}$ suggests that the reduction in $k^{A\to D}$ with applied dc field is due to the decrease in the number of energetically accessible Stark levels. However, the decrease in $k^{A\to D}$ is less than would be expected simply from consideration of N_A. A possible explanation for this may be found by noting that the Stark states that remain accessible are those states that have the greatest degree of spatial overlap with the parent states and by assuming that transitions to such states are favored. However, it is observed that, at applied fields where states from the $n=30$ and 31 manifolds overlap, mixing occurs simultaneously both to upper $n=30$ and lower $n=31$ states, which have very different spatial characteristics. This is not inconsistent with the wave function overlap considerations just presented because, as is evident from Fig. 1, the parent levels acquire the character of states associated with both manifolds in this field region.

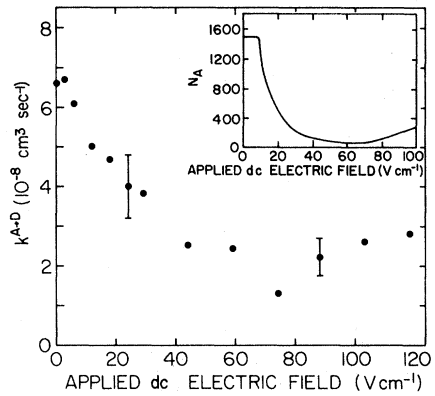

FIG. 5. Applied dc electric field dependence of $k^{A\to D}$ for parent Xe($31f$) atoms. The relative measurement error, shown at two values of the field, is ±20%. The total uncertainty in the absolute value of the measured rates is ±50%. The inset shows the number N_A of Stark states that lie within 0.9 cm^{-1} of the parent levels as a function of applied dc field.

The presence of an applied electric field thus leads to marked changes in both the final-state distribution resulting from thermal energy state changing collisions and in the rate constant for such processes.[22] These changes can be explained qualitatively using energy transfer arguments based on the essentially-free electron model, although the degree gree of spatial overlap between the wave functions associated with the initial and final states also appears to be important.

ACKNOWLEDGMENTS

We wish to thank N. F. Lane for many helpful discussions. This research was supported by the National Science Foundation under Grant No. PHY 78-09860 and by the Robert A. Welch Foundation.

[1]F. G. Kellert, K. A. Smith, R. D. Rundel, F. B. Dunning, and R. F. Stebbings, J. Chem. Phys. 72, 3179 (1980); Phys. Rev. Lett. 40, 1362 (1978).

[2]F. G. Kellert, C. Higgs, K. A. Smith, G. F. Hildebrandt, F. B. Dunning, and R. F. Stebbings, J. Chem. Phys. 72, 6312 (1980).

[3]C. Higgs, K. A. Smith, G. B. McMillian, F. B. Dunning, and R. F. Stebbings, J. Phys. B 14, L285 (1981).

[4]C. Higgs, K. A. Smith, F. B. Dunning, and R. F. Stebbings, J. Chem. Phys. 75, 745 (1981).

[5]F. G. Kellert, T. H. Jeys, G. B. McMillian, K. A. Smith, F. B. Dunning, and R. F. Stebbings, Phys. Rev. A 23, 1127 (1981).

[6]L. M. Humphrey, T. F. Gallagher, W. E. Cooke, and S. A. Edelstein, Phys. Rev. A 18, 1383 (1978).

[7]T. F. Gallagher and W. E. Cooke, Phys. Rev. A 19, 2161 (1979).

[8]T. F. Gallagher, G. A. Ruff, and K. A. Safinya, Phys. Rev. A 22, 843 (1980).

[9]Preliminary studies of state changing in the presence of an applied field have been described by: M. P. Slusher, C. Higgs, K. A. Smith, F. B. Dunning, and R. F. Stebbings, *Abstracts of the XII International Conference on the Physics of Electronic and Atomic Collisions, Gatlin-*

burg, Tennessee, 1981, edited by S. Datz (North-Holland, Amsterdam, 1981), p. 1111; F. Gounand, T. F. Gallagher, K. A. Safinya, and W. Sandner, *ibid.*, p. 1113.

[10]T. H. Jeys, G. W. Foltz, K. A. Smith, E. J. Beiting, F. G. Kellert, F. B. Dunning, and R. F. Stebbings, Phys. Rev. Lett. 44, 390 (1980).

[11]T. H. Jeys, G. B. McMillian, K. A. Smith, F. B. Dunning, and R. F. Stebbings, Phys. Rev. A 26, 335 (1982).

[12]G. B. McMillian, T. H. Jeys, K. A. Smith, F. B. Dunning, and R. F. Stebbings, J. Phys. B (in press).

[13]T. F. Gallagher and W. E. Cooke, Phys. Rev. A 19, 694 (1979).

[14]W. E. Cooke and T. F. Gallagher, Phys. Rev. A 17, 1226 (1978).

[15]J. H. M. Neijzen and A. Dönszelmann, J. Phys. B 15, L87 (1982).

[16]J. R. Rubbmark, M. M. Kash, M. G. Littman, and D. Kleppner, Phys. Rev. A 23, 3107 (1981).

[17]H. J. Silverstone, Phys. Rev. A 18, 1853 (1978).

[18]R. J. Damburg and V. V. Kolosov, J. Phys. B 12, 2637 (1979); 11, 1921 (1978); 9, 3149 (1976).

[19]See, for example, M. L. Zimmerman, M. G. Littman, M. M. Kash, and D. Kleppner, Phys. Rev. A 20, 2251 (1979).

[20]In near zero applied field changes in $|m_l|$ may occur due to precession in off-axis residual electric or magnetic fields. However, previous studies using the present apparatus show that application of a dc electric field $\gtrsim 3$ V cm^{-1} prevents any such effects. [M. P. Slusher, C. Higgs, K. A. Smith, F. B. Dunning, and R. F. Stebbings, J. Chem. Phys. 76, 5303 (1982).]

[21]See, for example, E. Fermi, Nuovo Cimento 11, 157 (1934); M. Matsuzawa, J. Phys. Soc. Jpn. 32, 1088 (1972); J. Phys. B 8, L382 (1975); 8, 2114 (1975); 10, 1543 (1977); M. R. Flannery, Phys. Rev. A 22, 2408 (1980); J. Phys. B 13, L657 (1980).

[22]Studies of Xe(24*f*)-Xe collisions showed effects, similar to those observed in Xe(31*f*)-Xe collisions, that could again be explained using the essentially-free electron model.